# Understanding Negative Samples in Instance Discriminative Self-supervised Representation Learning

Kento Nozawa
The University of Tokyo & RIKEN
nozawa.kento@gmail.com

Issei Sato
The University of Tokyo & RIKEN
sato@k.u-tokyo.ac.jp

December 23, 2024

#### **Abstract**

Instance discriminative self-supervised representation learning has been attracted attention thanks to its unsupervised nature and informative feature representation for downstream tasks. Self-supervised representation learning commonly uses more negative samples than the number of supervised classes in practice. However, there is an inconsistency in the existing analysis; theoretically, a large number of negative samples degrade supervised performance, while empirically, they improve the performance. We theoretically explain this empirical result regarding negative samples. We empirically confirm our analysis by conducting numerical experiments on CIFAR-10/100 datasets.

# 1 Introduction

Self-supervised representation learning is a popular class of unsupervised representation learning algorithms in the domains of vision [Bachman et al., 2019, Chen et al., 2020a, He et al., 2020, Caron et al., 2020, Grill et al., 2020] and text [Mikolov et al., 2013, Devlin et al., 2019, Brown et al., 2020]. Generally, self-supervised representation learning trains a feature extractor by solving a pretext task constructed on a large unlabeled dataset. The learned feature extractor yields generic feature representations for other machine learning tasks such as classification. Recent algorithms help a linear classifier to attain classification accuracy comparable to a supervised method from scratch, especially in a few amount of labeled data regime [Newell and Deng, 2020, Hénaff et al., 2020, Chen et al., 2020b]. For example, SwAV [Caron et al., 2020] with ResNet-50 has a top-1 validation accuracy of 75.3% on the ImageNet-1K classification [Deng et al., 2009] compared with 76.5% by using the fully supervised method.

InfoNCE [van den Oord et al., 2018] or its modification is a de facto standard objective used in many state-of-the-art self-supervised methods [Logeswaran and Lee, 2018, Bachman et al., 2019, He et al., 2020, Chen et al., 2020a, Hénaff et al., 2020, Caron et al., 2020]. Intuitively, the minimization of InfoNCE can be viewed as the minimization of cross-entropy loss on K+1 instance-wise classification, where K is the number of negative samples. Despite the empirical success of self-supervised learning, we still do not understand well why InfoNCE-based self-supervised learning algorithms perform well for downstream tasks.

Arora et al. [2019] propose the first theoretical framework for contrastive unsupervised representation learning (CURL). However, there exists a gap between the theoretical analysis and empirical observation as in Figure 1. Precisely, Arora et al. [2019] theoretically argue that a large number of negative samples degrade classification performance on a downstream task; however, a large number of negative samples tends to improve classification performance in practice [He et al., 2020, Chen et al., 2020a].

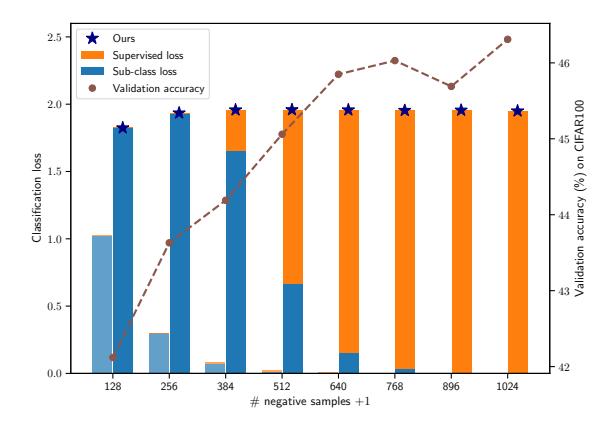


Figure 1: Validation accuracy and lower bounds of self-supervised representations learning on CIFAR-100. **Left bars**: The existing contrastive unsupervised representation learning bound [Arora et al., 2019] does not explain why validation accuracy improves when the number of negative samples increases. This is because the lower bound of self-supervised loss is dominant by a collision term that is not related to classification loss (see Eq. (8) for the definition). **Right bars with** \*: On the other hand, the proposed bound (10) likely to contain classification losses when the number of negative samples increases. Section 6 describes the details of this experiment.

**Contributions.** We theoretically show that the existing lower bound fails to explain why large negative samples empirically improve downstream performance in Section 3. We propose a novel lower bound to theoretically explain this empirical observation regarding negative samples in Section 4.

# 2 Preliminary: InfoNCE-based Self-supervised Representations Learning

We analyze a widely used self-supervised loss function called InfoNCE [van den Oord et al., 2018, Eq. 4]. InfoNCE-based loss is a de facto standard loss; state-of-the-art self-supervised representation learning algorithms minimize it or its modification [Bachman et al., 2019, He et al., 2020, Hénaff et al., 2020, Chen et al., 2020a, Caron et al., 2020].

In this work, we focus on Chen et al. [2020a]'s self-supervised representation learning formulation, namely, SimCLR. We can only access a training unlabeled dataset  $\{\mathbf{x}_i\}_{i=1}^N$ , where input  $\mathbf{x} \in \mathcal{X}$  and  $\mathcal{X}$  is an input space, e.g.,  $\mathbb{R}^{3 \times \text{width} \times \text{height}}$  for color images. SimCLR learns feature extractor  $\mathbf{f} : \mathcal{X} \to \mathbb{R}^h$  modeled by neural networks on the dataset, where h is the dimensionality of feature representation. Let  $\mathbf{z} = \mathbf{f}(\mathbf{a}(\mathbf{x}))$  be a feature representation of  $\mathbf{x}$  after applying data augmentation  $\mathbf{a}(\cdot)$ . Note that  $\mathbf{z}$  is normalized by its L2 norm. Data augmentation  $\mathbf{a}$  is a pre-defined stochastic function,  $\mathbf{a} : \mathcal{X} \to \mathcal{X}$ , such as a composition of the horizontal flipping and cropping. Let  $\mathbf{z}' = \mathbf{f}(\mathbf{a}'(\mathbf{x}))$  be another feature representation of the same sample  $\mathbf{x}$  with different data augmentation  $\mathbf{a}'(\cdot)$ .

SimCLR minimizes the following InfoNCE-based loss with K negative samples for each pair of  $(\mathbf{z}, \mathbf{z}')$ :

$$\ell_{\text{Info}}(\mathbf{z}, \mathbf{Z}) := -\ln \frac{\exp(\mathbf{z} \cdot \mathbf{z}'/t)}{\sum_{\mathbf{z}_k \in \mathbf{Z}} \exp(\mathbf{z} \cdot \mathbf{z}_k/t)},\tag{1}$$

where  $\mathbf{Z} = \{\mathbf{z}', \mathbf{z}_1^-, \dots, \mathbf{z}_K^-\}$  is positive representation  $\mathbf{z}'$  and K negative representations  $\{\mathbf{z}_1^-, \dots, \mathbf{z}_K^-\}$ 

created from other samples, (...) is an inner product of two representations, and  $t \in \mathbb{R}_+$  is a temperature parameter. In our analysis, we use temperature parameter t = 1 for simplicity, but our analysis holds with any temperature. Intuitively, this loss function approximates an instance-wise classification loss by using K random negative samples [Wu et al., 2018]. From the definition of Eq. (1), we expect that f learns an invariant encoder with respect to data augmentation a. After minimizing Eq. (1), f is used as a feature extractor for downstream tasks such as classification.

#### **Extension of Contrastive Unsupervised Representation Learning** 3 **Framework**

We focus on the direct relationship between the self-supervised loss and a supervised loss to understand the role of the number of negative samples K. For a similar problem setting, the CURL framework [Arora et al., 2019] shows the averaged supervised loss is bounded by the contrastive unsupervised loss. Thus, we extend the CURL's analysis to the self-supervised representation learning in Section 2, and then we point out the CURL bound fails to explain empirical observation with large negative samples as in Figure 1.

#### 3.1 CURL Formulation for SimCLR

By following the CURL analysis [Arora et al., 2019], we introduce two steps' learning process: selfsupervised representation learning step and supervised learning step.

#### 3.1.1 Self-supervised learning step

The purpose of the self-supervised learning step is to learn a feature extractor f on an unlabeled dataset. During this step, we can only access input samples from  $\mathcal{X}$  without any relationship between samples, unlike metric learning [Kulis, 2012] or SU learning [Bao et al., 2018].

We formulate the data generation process for Eq. (1). The key idea of the CURL analysis is the existence of latent classes C that are associated with supervised classes. Let  $\rho$  be a probability distribution over C, and let x be an input sample drawn from a data distribution  $D_c$  conditioned on a latent class  $c \in \mathcal{C}$ . We draw two data augmentations a, a' from the distribution of data augmentation  $\mathcal{A}$  and apply them independently to the sample. As a result, we have two augmented samples  $\mathbf{a}(\mathbf{x}), \mathbf{a}'(\mathbf{x})$  and we call  $\mathbf{a}'(\mathbf{x})$  as a positive sample of  $\mathbf{a}(\mathbf{x})$ . Similarly, we draw K negative samples from  $\mathcal{D}_{c_b^-}$  for each  $c_k^- \in \{c_1^-, \dots, c_K^-\} \sim \rho^K$  and K data augmentations from  $\mathcal{A}$ , and then we apply them to negative samples. Definition 1 is the summary.

### **Definition 1** (Data Generation Process).

- 1. Draw latent classes:  $c, \{c_k^-\}_{k=1}^K \sim \rho^{K+1}$ ;
- 2. Draw input sample:  $\mathbf{x} \sim \mathcal{D}_c$ ;
- 3. Draw data augmentations:  $\mathbf{a}, \mathbf{a}' \sim \mathcal{A}^2$ ;
- 4. Apply data augmentations:  $\mathbf{a}(\mathbf{x}), \mathbf{a}'(\mathbf{x})$ ;
- 5. Draw negative samples:  $\{\mathbf{x}_k^-\}_{k=1}^K \sim \mathcal{D}_{c_k^-}^K$ ;
  6. Draw data augmentations:  $\{\mathbf{a}_k^-\}_{k=1}^K \sim \mathcal{A}^K$ ;
- 7. Apply data augmentations:  $\{\mathbf{a}_k^-(\mathbf{x}_k^-)\}_{k=1}^K$ .

 $<sup>^{1}</sup>$ Technically, we do not need c to draw x. However, we explicitly include it in the data generation process to understand the relationship with a supervised task in Section 3.2.

Note that in the original CURL's data generation process, a positive sample of x is drawn from  $\mathcal{D}_c$  independently, and it does not use any data augmentations.

From the data generation process and InfoNCE loss (1), we give the formal definition of self-supervised loss as follows.

**Definition 2** (Self-supervised Loss). Expected self-supervised loss is defined as

$$L_{\text{Info}}(\mathbf{f}) := \underset{c, \{c_k^-\}_{k=1}^K \sim \rho^{K+1}}{\mathbb{E}} \underset{\mathbf{a}, \mathbf{a}' \sim \mathcal{A}^2}{\mathbb{E}} \underset{\{\mathbf{a}_k^-\}_{k=1}^K \sim \mathcal{A}^K}{\mathbb{E}} \ell_{\text{Info}}(\mathbf{z}, \mathbf{Z}).$$
(2)

Since we cannot directly minimize Eq. (2), we minimize the empirical counterpart,  $\hat{L}_{Info}(\mathbf{f})$ , by sampling from the training dataset. Learned  $\hat{\mathbf{f}}$  works as a feature extractor in the supervised learning step.

#### 3.1.2 Supervised learning step

At the supervised learning step, we can observe label  $y \in \mathcal{Y} = \{1, \dots, Y\}$  for each  $\mathbf{x}$  that is the same as in the self-supervised learning step. Let  $\mathcal{D} = \mathcal{X} \times \mathcal{Y}$  be a data distribution, and  $\mathbf{g} \circ \hat{\mathbf{f}} : \mathcal{X} \to \mathbb{R}^Y$  be a classifier, where  $\mathbf{g} : \mathbb{R}^h \to \mathbb{R}^Y$  and  $\hat{\mathbf{f}}$  is the frozen feature extractor. Given the test data distribution and classifier, our goal is to minimize the following supervised loss:

$$L_{\sup}(\mathbf{g} \circ \widehat{\mathbf{f}}) := \underset{\mathbf{a} \sim \mathcal{A}}{\mathbb{E}} - \ln \frac{\exp\left(\mathbf{g}(\widehat{\mathbf{f}}(\mathbf{a}(\mathbf{x})))_y\right)}{\sum_{j \in Y} \exp\left(\mathbf{g}(\widehat{\mathbf{f}}(\mathbf{a}(\mathbf{x})))_j\right)}.$$
 (3)

By following Arora et al. [2019]'s analysis, we introduce a mean classifier as a simpler instance of g because its loss is an upper bound of Eq. (3). The mean classifier is the linear classifier whose weight of label y is computed by averaging representations:  $\mu_y = \mathbb{E}_{x \sim \mathcal{D}_y} \mathbb{E}_{\mathbf{a} \sim \mathcal{A}} \mathbf{f}(\mathbf{a}(\mathbf{x}))$ , where  $\mathcal{D}_y$  is a data distribution conditioned on the supervise label y. We introduce the definition of the mean classifier's supervised loss as follows:

**Definition 3** (Mean Classifier's Supervised Loss).

$$L_{\sup}^{\mu}(\widehat{\mathbf{f}}) := \underset{\mathbf{a} \sim \mathcal{A}}{\mathbb{E}} - \ln \frac{\exp\left(\widehat{\mathbf{f}}(\mathbf{a}(\mathbf{x})) \cdot \boldsymbol{\mu}_{y}\right)}{\sum_{j \in \mathcal{Y}} \exp\left(\widehat{\mathbf{f}}(\mathbf{a}(\mathbf{x})) \cdot \boldsymbol{\mu}_{j}\right)}.$$
 (4)

We also introduce a sub-class loss function.<sup>2</sup> Let  $\mathcal{Y}_{\mathrm{sub}}$  be a subset of  $\mathcal{Y}$  and  $\mathcal{D}_{\mathrm{sub}}$  be a data distribution over  $\mathcal{X} \times \mathcal{Y}_{\mathrm{sub}}$ , then we define the mean classifier's sub-class loss:

**Definition 4** (Mean Classifier's Supervised Sub-class Loss).

$$L_{\text{sub}}^{\mu}(\widehat{\mathbf{f}}, \mathcal{Y}_{\text{sub}}) := \underset{\mathbf{x}, y \sim \mathcal{D}_{\text{sub}}}{\mathbb{E}} \ell_{\text{sub}}^{\mu}(\widehat{\mathbf{f}}(\mathbf{a}(\mathbf{x})), y, \mathcal{Y}_{\text{sub}}),$$

$$where \quad \ell_{\text{sub}}^{\mu}(\mathbf{z}, y, \mathcal{Y}_{\text{sub}}) := -\ln \frac{\exp(\mathbf{z} \cdot \boldsymbol{\mu}_{y})}{\sum_{j \in \mathcal{Y}_{\text{sub}}} \exp(\mathbf{z} \cdot \boldsymbol{\mu}_{j})}.$$

$$(5)$$

<sup>&</sup>lt;sup>2</sup>Arora et al. [2019] refer to this loss function as averaged supervised loss.

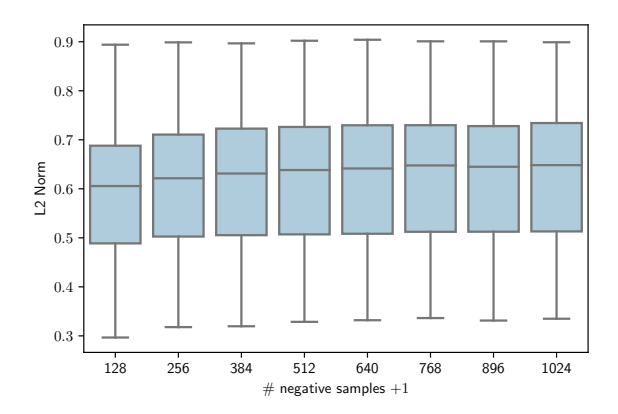


Figure 2: The boxplots of L2 norm of mean feature representations over the same supervised class on CIFAR-100. We used  $\|\mathbb{E}_{\mathbf{x}\sim\mathcal{D}_c}\mathbf{f}(\mathbf{x})\|_2^2$  as an approximation of  $\|\boldsymbol{\mu}_c\|_2^2$ .

The purpose of unsupervised representation learning [Bengio et al., 2013] is to learn generic feature representation rather than to improve the linear classifier's performance on the same dataset. However, we believe that such a feature extractor tends to transfer well to another task. In fact, Kornblith et al. [2019] empirically show a strong correlation between ImageNet's accuracy and transfer accuracy.

# 3.2 Theoretical Analysis by using CURL

We show Eq. (2) is an upper bound of the expected sub-class loss of the mean classifier.

**Step 1. Introduce a lower bound** We derive a lower bound of unsupervised loss  $L_{\rm Info}(\mathbf{f})$ .

$$L_{\text{Info}}(\mathbf{f}) \geq \underset{\substack{\mathbf{z} \\ \mathbf{x}_{k} > \mathcal{D}_{c} \\ \mathbf{a} \sim \mathcal{A} \\ \{\mathbf{x}_{k}^{-} \sim \mathcal{D}_{c_{k}^{-}}\}_{k=1}^{K}}} \mathbb{E}_{\text{Info}}\left(\mathbf{z}, \left\{\boldsymbol{\mu}(\mathbf{x}), \boldsymbol{\mu}(\mathbf{x}_{1}^{-}), \dots, \boldsymbol{\mu}(\mathbf{x}_{K}^{-})\right\}\right)$$

$$\geq \underset{\substack{\mathbf{z} \sim \mathcal{A} \\ \{\mathbf{x}_{k}^{-} \sim \mathcal{D}_{c_{k}^{-}}\}_{k=1}^{K} \\ \mathbf{x} \sim \mathcal{D}_{c}}} \mathbb{E}_{\mathbf{a} \sim \mathcal{A}} \ell_{\text{Info}}\left(\mathbf{z}, \left\{\boldsymbol{\mu}(\mathbf{x}), \boldsymbol{\mu}_{c_{1}^{-}}, \dots, \boldsymbol{\mu}_{c_{K}^{-}}\right\}\right)$$

$$\geq \underset{\substack{\mathbf{z} \sim \mathcal{D}_{c} \\ \mathbf{a} \sim \mathcal{A}}} \mathbb{E}_{\mathbf{a} \sim \mathcal{A}} \ell_{\text{Info}}\left(\mathbf{z}, \left\{\boldsymbol{\mu}_{c}, \boldsymbol{\mu}_{c_{1}^{-}}, \dots, \boldsymbol{\mu}_{c_{K}^{-}}\right\}\right) + d(\mathbf{f}),$$

$$\geq \underset{\substack{\mathbf{z} \sim \mathcal{D}_{c} \\ \mathbf{a} \sim \mathcal{A}}} \mathbb{E}_{\mathbf{a} \sim \mathcal{A}} \ell_{\mathbf{a} \sim \mathcal{A}} \ell_{\mathbf{a}$$

where  $\mu(\mathbf{x}) = \mathbb{E}_{\mathbf{a} \sim \mathcal{A}} \mathbf{f}(\mathbf{a}(\mathbf{x}))$  and  $d(\mathbf{f}) = \frac{1}{t} \mathbb{E}_{c \sim \rho} \left[ -\mathbb{E}_{\mathbf{x} \sim \mathcal{D}_c} \| \mu(\mathbf{x}) \|_2^2 \right]$ . The first and second inequalities are done by using Jensen's inequality for convex function. The proof of the third inequality is shown in Appendix A.1. We confirm that term d has a small absolute value in practice (see Tables 1 and 2).

**Remark 5.** We expect that the norm  $\|\mu(\mathbf{x})\|_2^2$  takes almost 1 and does not largely change even if the number of negative samples increases. This is because we learn transform invariant feature extractor  $\mathbf{f}$  and its L2 norm normalizes  $\mathbf{z}$ . Thus, if  $\|\mu_c\|_2^2$  takes a small value, i.e., almost 0,  $d(\mathbf{f})$  takes the minimum. However,  $\|\mu_c\|_2^2$  tends to increase by increasing the number of negative samples as in Figure 2 in practice.

Step 2. Decomposition into the averaged sub-class loss We convert the first term of Eq. (7) into the expected sub-class loss explicitly. By following Arora et al. [2019, Theorem B.1], we introduce collision probability:  $\tau_K = \mathbb{P}(\operatorname{Col}(c, \{c_k^-\}_{k=1}^K) \neq 0)$ , where  $\operatorname{Col}(c, \{c_k^-\}_{k=1}^K) = \sum_{k=1}^K \mathbb{I}[c = c_k^-]$  and  $\mathbb{I}$  is the indicator function. We omit the arguments of  $\operatorname{Col}$  for simplicity. Let  $\mathcal{C}_{\operatorname{sub}}(\{c, c_1^-, \dots, c_K^-\})$  be a function to remove duplicated latent classes given sampled latent classes. We omit the arguments of  $\mathcal{C}_{\operatorname{sub}}$  as well.

We decompose Eq. (7) into the expected sub-class loss and collision term by using  $\tau$ . The result is our extension of Arora et al. [2019, Lemma 4.3] for self-supervised representation learning as the following proposition:

Proposition 6 (CURL Lower Bound of Self-supervised Loss). For all f,

$$L_{\text{Info}}(\mathbf{f}) \ge (1 - \tau_K) \underset{c, \{c_k^-\}_{k=1}^K \sim \rho^{K+1}}{\mathbb{E}} \underbrace{\left[ \underbrace{L_{\text{sub}}^{\mu}(\mathbf{f}, \mathcal{C}_{\text{sub}})}_{\text{sub-class loss}} \mid \text{Col} = 0 \right]}_{\text{sub-class loss}} + \tau_K \underset{c, \{c_k^-\}_{k=1}^K \sim \rho^{K+1}}{\mathbb{E}} \underbrace{\left[ \ln(\text{Col} + 1)}_{\text{collision}} \mid \text{Col} \neq 0 \right] + d(\mathbf{f}).$$
(8)

The proof is found in Appendix A.2.

Arora et al. [2019] also show Rademacher complexity based generalization error bound for the mean classifier. Since we focus on the behavior of the self-supervised loss rather than a generalization error bound when K increases, we do not perform further analysis as was done in Arora et al. [2019]. Nevertheless, we believe that constructing a generalization error bound by following either Arora et al. [2019, Theorem 4.1] or Nozawa et al. [2020, Theorem 7] is worth interesting future work.

## 3.3 Limitations of Eq. (8)

The bound (8) tells us that K gives a trade-off between the sub-class loss and collision term via  $\tau_K$ . Recall that our final goal is to minimize Eq. (4) rather than expected Eq. (5). To incorporate the original supervised loss (4) into Eq. (8), we need K large enough to satisfy  $\mathcal{C}_{\text{sub}} \supseteq \mathcal{Y}$ . However, such a large K makes the lower bound meaningless.

We can easily observe that the lower bound converges to the collision term by increasing K since the collision probability  $\tau_K$  converges to 1. As a result, the sub-class loss rarely contributes to the lower bound. Let us consider the bound on CIFAR-10, where the number of supervised classes is 10, and latent classes are the same as the supervised classes. When  $\tau_{K=32}\approx 0.967$ , i.e., the only 3.4% training samples contribute to the expected sub-class loss, the others fall into the collision term. Indeed, Arora et al. [2019] theoretically and empirically argue that large negative samples degrade classification performance of the expected sub-class task in the CURL setting. However, even much larger negative samples, for example, K+1=512, yield the best performance of a linear classifier with self-supervised representation on CIFAR-10 [Chen et al., 2020a, Figure B.7].

# 4 Proposed Lower Bound for Instance-wise Self-supervised Representation Learning

To fill the gap between the theoretical bound and empirical observation from recent work, we propose another lower bound for self-supervised representation learning. The key idea of our bound is to replace  $\tau$  with a different probability since  $\tau$  can easily increase depending on K. We also focus on the supervised loss rather than the expected sub-class loss.

# 4.1 Proposed Lower Bound

Let  $v_K$  be a probability such that sampled K latent classes contain all latent classes:  $\{c_k\}_{k=1}^K \supseteq \mathcal{C}$ . This probability is treated in the coupon collector's problem of probability theory (e.g., Durrett [2019, Example 2.2.7]). If the latent class's probability is uniform:  $\forall c, \rho(c) = 1/|\mathcal{C}|$ , then we can calculate the probability explicitly as follows.

**Definition 7** (Probability to Draw All Latent Classes). Assume that  $\rho$  is a uniform distribution over latent classes C. The probability such that drawn K latent classes from  $\rho$  contain all latent classes is defined as

$$v_K := \sum_{n=1}^K \sum_{m=0}^{|\mathcal{C}|-1} \binom{|\mathcal{C}|-1}{m} (-1)^m \left(1 - \frac{m+1}{|\mathcal{C}|}\right)^{n-1},\tag{9}$$

where the first summation is a probability such that n drawn latent samples contain all latent classes [Nakata and Kubo, 2006, Eq. 2].<sup>3</sup>

By using Eq. (9) instead of  $\tau$ , we show our lower bound of self-supervised loss:

**Theorem 8** (Lower Bound of Self-supervised Loss). Given Eq. (9),  $\forall \mathbf{f}$ ,

$$L_{\text{Info}}(\mathbf{f}) \geq \frac{1}{2} \left\{ v_{K+1} \underset{c, \{c_k^-\}_{k=1}^K \sim \rho^{K+1}}{\mathbb{E}} \underbrace{\left[ \underbrace{L_{\text{sub}}^{\mu}(\mathbf{f}, \mathcal{C})}_{\text{sup. loss: } L_{\text{sup}}^{\mu}} \mid \mathcal{C}_{\text{sub}} = \mathcal{C} \right] \right.$$

$$+ \left. (1 - v_{K+1}) \underset{c, \{c_k^-\}_{k=1}^K \sim \rho^{K+1}}{\mathbb{E}} \underbrace{\left[ \underbrace{L_{\text{sub}}^{\mu}(\mathbf{f}, \mathcal{C}_{\text{sub}})}_{\text{sub-class loss}} \mid \mathcal{C}_{\text{sub}} \neq \mathcal{C} \right] \right.$$

$$+ \underbrace{\mathbb{E}}_{c, \{c_k^-\}_{k=1}^K \sim \rho^{K+1}} \underbrace{\ln(\text{Col} + 1)}_{\text{collision}} \right\} + d(\mathbf{f}).$$

$$(10)$$

The proof is found in Appendix A.3.

Theorem 8 tells us that probability  $v_{K+1}$  converges to 1 by increasing the number of negative samples K; as a result, the self-supervised loss is more likely to contain the supervised loss and the collision term. The sub-class loss contributes to the self-supervised loss when K is small as in Eq. (8). Let us consider the concrete value of v with the same setting discussed in Section 3.3. When  $v_{K=32}\approx 0.719$ , i.e., the 71.9% training samples contribute the supervised loss.

During the minimization of  $L_{\rm Info}$ , we cannot minimize  $L_{\rm sup}^{\mu}$  in Eq. (10) directly since we cannot access supervised and latent classes. However, we find a similar formulation in clustering-based self-supervised representation learning algorithms that use pseudo-class by performing unsupervised clustering.

**Remark 9.** Clustering-based self-supervised representation learning algorithms, such as  $DeepCluster[Caron\ et\ al.,\ 2018]$ ,  $SwAV[Caron\ et\ al.,\ 2020]$ , and  $PCL[Li\ et\ al.,\ 2021]$ , use prototype representations instead of  $\mathbf{z}', \{\mathbf{z}_k^-\}_{k=1}^K$  by applying unsupervised clustering on feature representations. This procedure is justified as the approximation of latent class's mean representation  $\mu_c$  with prototype representation to minimize the supervised loss in Eq. (10) rather than Eq. (1).

This replacement suggests that clustering-based algorithms perform well with a small mini-batch setting in practice [Caron et al., 2020].

 $<sup>^3</sup>$ We also show the expected K+1 to draw the all latent class for CIFAR-10, CIFAR-100, and ImageNet-1K in Appendix B.

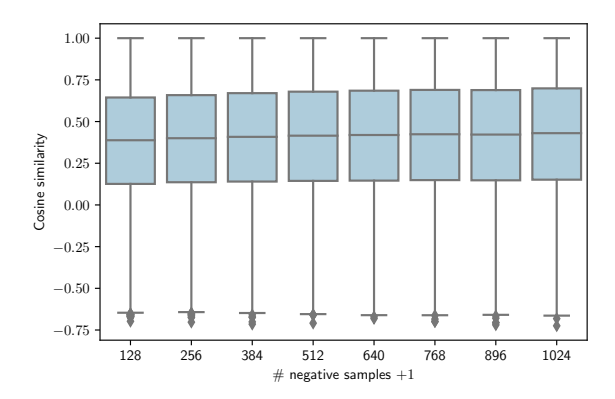


Figure 3: Cosine similarity between all pairs of feature representation in the same supervised class on CIFAR-100. We use feature representation  $\mathbf{f}(\mathbf{x})$  on the training dataset of CIFAR-100 to calculate cosine similarity. We confirm that the cosine similarity values do not change by increasing the number of negative samples in practice.

# **4.2** Large K does not Spread Features within Same Latent Class

We argue that the feature representations do not have a large within-class variance on the feature space by increasing K in practice. We show the upper bound of the collision term in the lower bounds to understand the effect of large negative samples.

**Corollary 10** (Upper Bound of the Collision Term). There exist non-negative constants  $\alpha$  and  $\beta$  only depending on the number of duplicated latent classes  $\operatorname{Col}(c,\{c_k^-\}_{k=1}^K)$  such that for fixed c and f, the collision term is bounded by

$$\alpha + \beta s(\mathbf{f}),$$
where  $s(\mathbf{f}) \coloneqq \mathbb{E}_{\substack{\mathbf{x} \sim \mathcal{D}_c \\ \mathbf{a}, \mathbf{a}' \sim \mathcal{A}^2}} \mathbb{E}_{\mathbf{a}^- \sim \mathcal{A}} |\mathbf{f}(\mathbf{a}(\mathbf{x})) \cdot [\mathbf{f}(\mathbf{a}^-(\mathbf{x}^-)) - \mathbf{f}(\mathbf{a}'(\mathbf{x}))]|,$ 

$$(11)$$

The proof is found in Appendix A.4. A similar upper bound is shown in Arora et al. [2019, Lemma 4.4]. Intuitively, we expect that two feature representations in the same latent class tend to be dissimiar by increasing K.

However,  $s(\mathbf{f})$  converges even if K is small in practice. Let us consider the condition when this upper bound achieves the maximum. Since  $\mathbf{f}(\mathbf{a}(\mathbf{x}))$  and  $\mathbf{f}(\mathbf{a}'(\mathbf{x}))$  are computed from the same input sample with different data augmentations, their inner product tends to be large positive; thus,  $\mathbf{f}(\mathbf{a}^-(\mathbf{x}^-))$  is located in the opposite direction of  $\mathbf{f}(\mathbf{a}(\mathbf{x}))$ . But, it is not possible to learn such representations because of the definition of InfoNCE with normalized representation and the dimensionality of feature space: Equilateral dimension. In fact, we empirically confirm that the cosine similarities within the same supervised class do not decrease (See Figure 3).

# 5 Modifications of SimCLR's Objective

Practically, feature extractor  ${\bf f}$  is a deep neural network, and it is optimized by using stochastic gradient descent or its variant. For each data sample in a mini-batch of size K+1, we treat the other samples as negative samples, and then we apply two data augmentations to each sample; as a result, we have 2K+2

To generalize *NT-Xent* with respect to the number of data augmentations A, we denote  $\mathbf{z}_{i,j}$  as a feature representation of  $i^{\text{th}}$  sample's with  $j^{\text{th}}$  data augmentation. The generalized loss function is defined by

$$\frac{1}{(K+1)A(A-1)} \sum_{i=1}^{K+1} \sum_{j=1}^{A} \sum_{l \neq j}^{A} \ell(i,j,l),$$
where 
$$\ell(i,j,l) = -\ln \frac{\exp\left(\mathbf{z}_{i,j} \cdot \mathbf{z}_{i,l}\right)}{\exp(\mathbf{z}_{i,j} \cdot \mathbf{z}_{i,l}) + \sum_{k \neq i}^{K+1} \sum_{a=1}^{A} \exp\left(\mathbf{z}_{i,j} \cdot \mathbf{z}_{k,a}^{-}\right)}.$$
(12)

Note that the number of negative samples is AK. Similar loss is proposed in Caron et al. [2020, Appendix A3.] for multiple cropped images.

As shown in our analysis, the number of negative sample K is associated with the number of latent classes. However, since AK negative samples come from at most K distinct latent classes in Eq. (12), the other different augmented negative samples might be redundant. Thus, we propose an alternative loss function with multiple augmented setting.

The proposed loss is viewed as an empirical approximation of Eq. (6). As an empirical approximation of  $\mu(\mathbf{x})$ , we introduce  $\mathbf{z}'_{i,j} = \frac{1}{A-1} \sum_{l \neq j}^{A} \mathbf{z}_{i,l}$  and  $\mathbf{z}_k^- = \frac{1}{A} \sum_{a=1}^{A} \mathbf{z}_{k,a}^-$ . The proposed loss is defined by

$$\frac{1}{A(K+1)} \sum_{i=1}^{K+1} \sum_{j=1}^{A} \ell(i,j), \tag{13}$$
where 
$$\ell(i,j) = -\ln \frac{\exp(\mathbf{z}_{i,j} \cdot \mathbf{z}'_{i,j})}{\exp(\mathbf{z}_{i,j} \cdot \mathbf{z}'_{i,j}) + \sum_{k \neq i}^{K+1} \exp(\mathbf{z}_{i,j} \cdot \mathbf{z}_{k}^{-})}.$$

We refer this loss function as averaged NT-Xent, namely, ANT-Xent. We find that the evaluation cost of Eq. (13) is slightly lower than Eq. (12) since the number of negative samples is K instead of AK.

We propose another modification, namely, *NAT-Xent*. Unlike normalized feature  $\mathbf{z}$ , the others,  $\mathbf{z}'$ ,  $\mathbf{z}^-$ , are unnormalized feature representations in Eq. (13). As suggested by Chen et al. [2020a], normalization in *NT-Xent* is a key technique to improve performance in practice. Therefore, we swap the order of average and normalization for both  $\mathbf{z}'$  and  $\mathbf{z}^-$ ; we normalize averaged feature representation over the different data augmentations. Note that since the cosine similarity is neither convex nor concave function, *NAT-Xent* might not be a lower bound of  $L_{Info}$ .

# 6 Experiments

We numerically compared our theoretical bound and CURL extension by using SimCLR [Chen et al., 2020a] on the image classification task. We used datasets with a relatively small number of classes to compare the existing bound and the proposed bound.

<sup>&</sup>lt;sup>4</sup>It stand for *Normalized Temperature-scaled Cross-entropy*.

**Datasets and Data Augmentations** We used the CIFAR-10 and CIFAR-100 [Krizhevsky, 2009] image classification datasets with the original  $50\,000$  training samples for both self-supervised and supervised training and the original 10,000 validation samples for the evaluation of supervised learning. We used the same data augmentations in the CIFAR-10 experiment provided by Chen et al. [2020a]: random resize cropping with the original image size, horizontal flipping with probability 0.5, color jitter with a strength parameter of 0.5 with probability 0.8, and grey scaling with probability 0.2.

**Self-supervised Learning** We mainly followed the experimental setting provided by Chen et al. [2020a] and its implementation<sup>5</sup>. We used ResNet-18 [He et al., 2016] as a feature encoder without the last fully connected layer. We replaced the first convolution layer with the convolutional layer with 64 output channels, the stride size of 1, the kernel size of 3, and the padding size of 3. We removed the first max-pooling from the encoder, and we added a non-linear projection head to the end of the encoder. The projection head consisted of the fully connected layer with 512 units, batch-normalization [Ioffe and Szegedy, 2015], ReLU activation function, and another fully-connected layer with 128 units and without bias.

We trained the encoder by using PyTorch [Paszke et al., 2019]'s distributed data-parallel training on four GPUs that are NVIDIA Tesla P100. For distributed training, we replaced all batch-normalization with synchronized batch-normalization. We used stochastic gradient descent with momentum factor of 0.9 on 500 epochs. We used LARC [You et al., 2017], and its global learning rate was updated by using linear warmup at each step during the first 10 epochs, then updated by using cosine annealing without restart [Loshchilov and Hutter, 2017] at each step until the end. We initialized the learning rate with (K+1)/256. We applied weight decay of  $10^{-4}$  to all weights excepts for parameters of all synchronized batch-normalization and bias terms. The temperature parameter was set to t=0.5 by default.

**Linear Evaluation** We report the validation accuracy of two linear classifiers: mean classifier and linear classifier. We constructed a mean classifier by averaging the feature representations of **z** per supervised class. We applied one data augmentation to each training sample, where the data augmentation is the same as in that the self-supervised learning step. For linear classifier **g**, we optimized **g** by using stochastic gradient descent with Nesterov's momentum[Sutskever et al., 2013] whose factor is 0.9 with 100 epochs. Similar to self-supervised training, we trained the classifier by using distributed data-parallel training on the four GPUs with 512 mini-batches on each GPU. The initial learning rate was 0.3 which was updated by using cosine annealing without restart [Loshchilov and Hutter, 2017] until the end.

**Bound Evaluation Procedure** We compared CURL's extension bound (8) and our bound (10) when we varied the number of negative samples K. We selected  $K+1 \in \{32, 64, 128, 256, 512\}$  for CIFAR-10 and  $K+1 \in \{128, 256, 384, 512, 640, 786, 896, 1024\}$  for CIFAR-100. We learned  $\hat{\mathbf{f}}$  by minimizing Eq. (12) with A=2. Then we approximated  $\mu_c$  by averaging 10 sampled data augmentations per sample on the training dataset, and we evaluated Equations (8) and (10) with the same negative sample size K as in self-supervised training. We reported the averaged values over validation samples with 10 epochs:  $(|10\,000/(K+1)| \times (K+1) \times \text{epoch})$  pairs of  $(\mathbf{z}, \mathbf{Z})$ .

**Loss Comparison** We empirically compared the three types of loss functions discussed in Section 5. For each loss function, we trained the encoder with a different temperature  $t \in \{0.1, 0.25, 0.5\}$  and the different number of data augmentations  $A \in \{2,3\}$  with K+1=512. We evaluated the validation accuracy of the linear classifier. In addition, we evaluated the validation accuracy with a practical manner [Chen et al., 2020a,c], where the projection head in **f** was removed after self-supervised learning to extract feature representations. We denoted the linear classifier with/without projection as "w/ head" and "w/o

<sup>5</sup>https://github.com/google-research/simclr

Table 1: The bound values on CIFAR-10 experiments with different K + 1. CURL bound, and its quantities represent with  $\dagger$ , and proposed ones represent without  $\dagger$ . The proposed collision values are half of  $\dagger$  collision.

K+1	32	64	128	256	512
$\mu$ acc	72.60	75.20	77.48	78.63	80.21
Linear acc	77.14	79.71	81.64	82.82	83.93
$L_{ m Info}$	2.02	2.64	3.29	3.96	4.64
d	-1.16	-1.17	-1.18	-1.18	-1.19
†Collision	1.32	1.93	2.59	3.26	3.94
†Bound	0.23	0.76	1.41	2.08	2.75
$^\dagger L^\mu_{ m sup}$	0.05	0.00	0.00	0.00	0.00
$^\dagger L_{ m sub}^{ ilde{\mu}^{ m r}}$	0.01	0.00	0.00	0.00	0.00
Bound	0.39	0.70	1.02	1.35	1.69
$L^{\mu}_{ m sup}$	0.63	0.90	0.91	0.90	0.91
$L_{ m sub}^{ ilde{\mu}^{-r}}$	0.26	0.01	0.00	0.00	0.00

head", respectively. We ran both self-supervised learning and linear evaluation three times with different random seeds and evaluated the averaged accuracy over three runs where each accuracy was the best one in different t.

As a reference of performance, we also trained a fully supervised model by using the same ResNet-18 without projection head and with a fully connected layer. All hyper-parameters, optimization procedure, and data augmentations were the exact same as those of the self-supervised learning experiments except for weight decay applied to all training parameters.

### 6.1 Experimental Results

Tables 1 and 2 show the bound values on CIFAR-10 and CIFAR-100, respectively. We also reported mean and linear classifiers' validation accuracy as " $\mu$  acc" and "Linear acc", respectively. We confirmed that CURL bounds converged to <sup>†</sup>Collision when a relatively small K. On the other hand, proposed bound values had still a large proportion of supervised loss  $L^{\mu}_{\sup}$  with larger K. Note that since the CURL bound does not contain  $^{\dagger}L^{\mu}_{\sup}$  explicitly in Eq. (8), we subtracted  $^{\dagger}L^{\mu}_{\sup}$  from  $^{\dagger}L^{\mu}_{\sup}$  in Eq. (8) and reported  $^{\dagger}L^{\mu}_{\sup}$  and subtracted  $^{\dagger}L^{\mu}_{\sup}$  for the comparison. Figure 1 shows the linear accuracy and the sum of the supervised and sub-class losses in existing and the proposed bounds.

Figures 4a and 4b show the proportion of  $d(\mathbf{f})$  in bounds on CIFAR-10 and CIFAR-100, respectively. The bound values are same as in Tables 1 and 2. Since  $d(\mathbf{f})$  takes a negative value as shown in Appendix A.1, we calculate the proportion  $\frac{|d(\mathbf{f})|}{\mathrm{Bound}+|d(\mathbf{f})|}$ , where the bound term is either Eq. (8) or Eq. (10). It is worth noting that the bounds without  $d(\mathbf{f})$  were still lower than  $L_{\mathrm{Info}}(\mathbf{f})$  in Tables 1 and 2.

Even our bound contains only sub-class loss  $L^{\mu}_{\mathrm{sub}}$  when K is relatively small; for example, regarding  $K+1 \in \{128,256\}$  on CIFAR-100, the validation accuracy of the classifiers surprisingly tends to be higher than the chance rate. Similar empirical results are reported in the contrastive learning setting by Arora et al. [2019]. However, we cannot theoretically explain this regime's generalization yet.

Table 3 shows the comparison of the linear evaluation performance with different A. The proposed losses, ANT-Xent and NAT-Xent achieved competitive performance with NT-Xent (12).

Table 2: The bound values on CIFAR-100 experiments with different K+1. CURL bound, and its quantities represent with  $\dagger$ , and proposed ones represent without  $\dagger$ . The proposed collision value is half of  $\dagger$  collision.

K+1	128	256	384	512	640	768	896	1024
$\mu$ acc	32.73	34.37	35.16	35.90	36.67	37.40	36.86	37.68
Linear acc	42.12	43.63	44.19	45.06	45.85	46.03	45.69	46.31
$L_{ m Info}$	3.31	3.98	4.38	4.66	4.88	5.06	5.21	5.34
d	-1.00	-0.99	-0.98	-0.97	-0.96	-0.95	-0.96	-0.95
†Collision	0.69	1.15	1.48	1.73	1.93	2.10	2.24	2.37
†Bound	0.72	0.46	0.58	0.78	0.98	1.15	1.29	1.42
$^\dagger L^\mu_{ m sup}$	0.00	0.00	0.01	0.01	0.00	0.00	0.00	0.00
$^{\dagger}L_{\mathrm{sub}}^{\overset{\mathrm{sup}}{\mu}}$	1.02	0.30	0.07	0.01	0.00	0.00	0.00	0.00
Bound	1.17	1.52	1.72	1.86	1.96	2.05	2.12	2.19
$L^{\mu}_{ m sup}$	0.00	0.00	0.30	1.29	1.80	1.92	1.96	1.95
$L_{ m sub}^{ ilde{\mu}^{ m p}}$	1.82	1.93	1.65	0.67	0.16	0.03	0.00	0.00

Table 3: The comparison of validation accuracy of linear classifiers with different self-supervised loss functions.

Dataset	A	NT-Xent [Chenw/o head	et al., 2020a] w/ head	ANT-Xen w/o head	t (Ours) w/ head	NAT-Xen w/o head	t (Ours) w/ head	Supervised
CIFAR-10	2 3	88.41 89.29	85.77 87.43	88.32 89.18	85.37 87.03	88.35 89.40	85.60 87.20	93.29
CIFAR-100	$\frac{2}{3}$	61.18 $62.52$	51.44 53.20	61.03 $62.14$	50.84 $52.71$	60.90 $62.01$	51.30 53.39	71.66

# 7 Related Work

# 7.1 Self-supervised Representation Learning

Self-supervised learning tries to learn an encoder that extracts generic feature representations from an unlabeled dataset. Self-supervised learning algorithms solve a pretext task that does not require any supervision and can be easily constructed on the dataset, such as denoising [Vincent et al., 2008], colorization [Zhang et al., 2016, Larsson et al., 2016] solving jigsaw puzzles [Noroozi and Favaro, 2016], inpainting blank pixels [Pathak et al., 2016], reconstructing missing channels [Zhang et al., 2017], predicting rotation [Gidaris et al., 2018], and adversarial generative models [Donahue and Simonyan, 2019] for vision; predicting neighbor words [Mikolov et al., 2013], generating neighbor sentences [Kiros et al., 2015], and solving masked language model [Devlin et al., 2019] for natural language processing.

Recent self-supervised learning algorithms for the vision domain mainly solve an instance discrimination task. Exemplar-CNN [Dosovitskiy et al., 2014] is one of the earlier algorithms that can obtain generic feature representations of images by using convolutional neural networks and data augmentation. van den Oord et al. [2018] proposed noise-contrastive estimation (NCE) [Gutmann and Hyvärinen, 2012] based loss function refereed to as InfoNCE. Then, many self-supervised algorithms minimize the InfoNCE-based objective, e.g., CPCv2 [Hénaff et al., 2020], DeepInfoMax [Hjelm et al., 2019], AMDIM [Bachman et al., 2019], MoCo [He et al., 2020], SwAV [Caron et al., 2020], and SimCLR [Chen et al., 2020a]. These feature representation learning algorithms boost supervised learning with few labeled

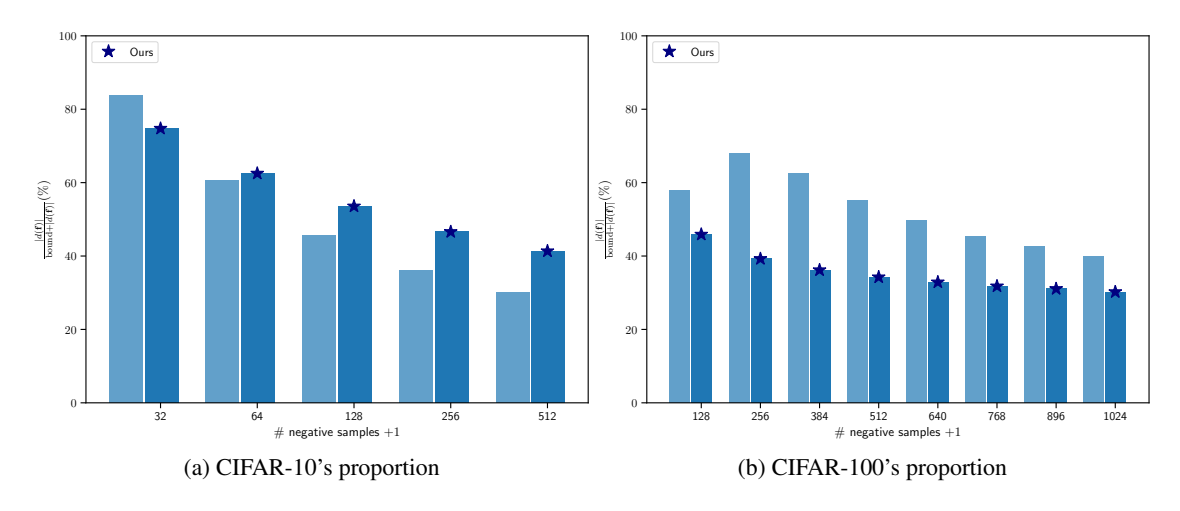


Figure 4: The proportion of  $d(\mathbf{f})$  in the bounds. The proportion tends to be smaller with larger negative samples.

data and semi-supervised learning performance [Chen et al., 2020b].

# 7.2 Theoretical Perspective

InfoNCE was initially proposed as a lower bound of intractable mutual information between feature representations [van den Oord et al., 2018, Poole et al., 2019] by using NCE. Optimizing the InfoNCE-based loss function can be considered as maximizing the InfoMax principle [Linsker, 1988]. The history of InfoMax-based self-supervised representation learning dates back to more than 30 years ago [Hinton and Becker, 1990]. However, this interpretation does not directly explain the generalization on a downstream task. In fact, Tschannen et al. [2020] empirically showed that the performances of classification on downstream tasks and mutual information estimation are uncorrelated with each other, and Kolesnikov et al. [2019] also reported a similar relationship between the performances of linear classification on downstream tasks and of pretext tasks. McAllester and Stratos [2020] theoretically showed the limitation of maximizing the lower bounds of mutual information – accurate approximation requires an exponential sample size.

Arora et al. [2019] give the first theoretical analyses to explain the generalization of the CURL. This analysis is the most related to our analysis. It is worth noting that our analysis focuses on the different representation learning setting, and we point out the limitation of the CURL when the number of negative samples increases.

Bansal et al. [2021] decomposed the generalization error gap of the *linear classifier* with feature representations trained on the same dataset. Wang and Isola [2020] decomposed the self-supervised loss into alignment and uniformity and showed properties of both metrics. Tosh et al. [2020] also analyzed self-supervised loss for augmented samples, but they only focused on one negative sample setting. Recently, Wei et al. [2021] propose learning theoretical analysis by introducing "expansion" assumption for self-training where (pseudo) labels are generated from the previously learned model. Learning theory-based analyses was also proposed for other types of self-supervised learning problem such as reconstruction tasks [Lee et al., 2020] and language modeling [Saunshi et al., 2021].

# 8 Conclusion

We theoretically pointed out the existing framework cannot explain why large negative samples did not degrade performance in practice, and we proposed a novel lower bound of a widely used self-supervised loss to explain the phenomenon.

We do not discuss properties of data augmentation explicitly in this work. Thus applying techniques used in the recent learning theoretical analyses [Chen et al., 2020d, Wei et al., 2021] with data augmentation might be a fruitful exploration to future work.

## References

- Sanjeev Arora, Hrishikesh Khandeparkar, Mikhail Khodak, Orestis Plevrakis, and Nikunj Saunshi. A Theoretical Analysis of Contrastive Unsupervised Representation Learning. In *ICML*, pages 5628–5637, 2019.
- Philip Bachman, R Devon Hjelm, and William Buchwalter. Learning Representations by Maximizing Mutual Information Across Views. In *NeurIPS*, pages 15535–15545, 2019.
- Ting Chen, Simon Kornblith, Mohammad Norouzi, and Geoffrey Hinton. A Simple Framework for Contrastive Learning of Visual Representations. In *ICML*, 2020a.
- Kaiming He, Haoqi Fan, Yuxin Wu, Saining Xie, and Ross Girshick. Momentum Contrast for Unsupervised Visual Representation Learning. In *CVPR*, pages 9726–9735, 2020.
- Mathilde Caron, Ishan Misra, Julien Mairal, Priya Goyal, Piotr Bojanowski, and Armand Joulin. Unsupervised Learning of Visual Features by Contrasting Cluster Assignments. In *NeurIPS*, 2020.
- Jean-Bastien Grill, Florian Strub, Florent Altché, Corentin Tallec, Pierre H. Richemond, Elena Buchatskaya, Carl Doersch, Bernardo Avila Pires, Zhaohan Daniel Guo, Mohammad Gheshlaghi Azar, Bilal Piot, Koray Kavukcuoglu, Rémi Munos, and Michal Valko. Bootstrap Your Own Latent A New Approach to Self-Supervised Learning. In *NeurIPS*, 2020.
- Tomas Mikolov, Ilya Sutskever, Kai Chen, Greg Corrado, and Jeffrey Dean. Distributed Representations of Words and Phrases and their Compositionality. In *NeurIPS*, pages 3111–3119, 2013.
- Jacob Devlin, Ming-Wei Chang, Kenton Lee, and Kristina Toutanova. BERT: Pre-training of Deep Bidirectional Transformers for Language Understanding. In *NAACL-HLT*, pages 4171–4186, 2019.
- Tom B. Brown, Benjamin Mann, Nick Ryder, Melanie Subbiah, Jared Kaplan, Prafulla Dhariwal, Arvind Neelakantan, Pranav Shyam, Girish Sastry, Amanda Askell, Sandhini Agarwal, Ariel Herbert-Voss, Gretchen Krueger, Tom Henighan, Rewon Child, Aditya Ramesh, Daniel M. Ziegler, Jeffrey Wu, Clemens Winter, Christopher Hesse, Mark Chen, Eric Sigler, Mateusz Litwin, Scott Gray, Benjamin Chess, Jack Clark, Christopher Berner, Sam Mccandlish, Alec Radford, Ilya Sutskever, and Dario Amodei. Language Models are Few-Shot Learners. In *NeurIPS*, 2020.
- Alejandro Newell and Jia Deng. How Useful is Self-Supervised Pretraining for Visual Tasks? In *CVPR*, pages 7345–7354, 2020.
- Olivier J. Hénaff, Aravind Srinivas, Jeffrey De Fauw, Ali Razavi, Carl Doersch, S. M. Ali Eslami, and Aaron Van den oord. Data-Efficient Image Recognition with Contrastive Predictive Coding. In *ICML*, pages 4182–4192, 2020.

- Ting Chen, Simon Kornblith, Kevin Swersky, Mohammad Norouzi, and Geoffrey Hinton. Big Self-Supervised Models are Strong Semi-Supervised Learners. In *NeurIPS*, 2020b.
- Jia Deng, Wei Dong, Richard Socher, Li-Jia Li, Kai Li, and Li Fei-Fei. ImageNet: A Large-Scale Hierarchical Image Database. In *CVPR*, pages 248–255, 2009.
- Aaron van den Oord, Yazhe Li, and Oriol Vinyals. Representation Learning with Contrastive Predictive Coding. *arXiv:1807.03748v2 [cs.LG]*, 2018.
- Lajanugen Logeswaran and Honglak Lee. An Efficient Framework for Learning Sentence Representations. In *ICLR*, 2018.
- Zhirong Wu, Yuanjun Xiong, Stella X. Yu, and Dahua Lin. Unsupervised Feature Learning via Non-Parametric Instance Discrimination. In *CVPR*, pages 3733–3742, 2018.
- Brian Kulis. Metric Learning: A Survey. *Foundations and Trends® in Machine Learning*, 5(4):287–364, 2012.
- Han Bao, Gang Niu, and Masashi Sugiyama. Classification from Pairwise Similarity and Unlabeled Data. In *ICML*, pages 452–461, 2018.
- Yoshua Bengio, Aaron Courville, and Pascal Vincent. Representation Learning: A Review and New Perspectives. *IEEE Transactions on Pattern Analysis and Machine Intelligence*, 35(8):1798–1828, 2013.
- Simon Kornblith, Jonathon Shlens, and Quoc V. Le. Do Better ImageNet Models Transfer Better? In *CVPR*, pages 2661–2671, 2019.
- Kento Nozawa, Pascal Germain, and Benjamin Guedj. PAC-Bayesian Contrastive Unsupervised Representation Learning. In *UAI*, pages 21–30, 2020.
- Rick Durrett. *Probability: Theory and Examples*. Cambridge Series in Statistical and Probabilistic Mathematics. Cambridge University Press, 5 edition, 2019.
- Toshio Nakata and Izumi Kubo. A Coupon Collector's Problem with Bonuses. In *Fourth Colloquium on Mathematics and Computer Science*, pages 215–224, 2006.
- Mathilde Caron, Piotr Bojanowski, Armand Joulin, and Matthijs Douze. Deep Clustering for Unsupervised Learning of Visual Features. In *ECCV*, pages 139–156, 2018.
- Junnan Li, Pan Zhou, Caiming Xiong, Richard Socher, and Steven C.H. Hoi. Prototypical Contrastive Learning of Unsupervised Representations. In *ICLR*, 2021.
- Mang Ye, Xu Zhang, Pong C. Yuen, and Shih-Fu Chang. Unsupervised Embedding Learning via Invariant and Spreading Instance Feature. In *CVPR*, pages 6210–6219, 2019.
- Alex Krizhevsky. Learning Multiple Layers of Features from Tiny Images. Technical report, 2009.
- Kaiming He, Xiangyu Zhang, Shaoqing Ren, and Jian Sun. Deep Residual Learning for Image Recognition. In *CVPR*, pages 770–778, 2016.
- Sergey Ioffe and Christian Szegedy. Batch Normalization: Accelerating Deep Network Training by Reducing Internal Covariate Shift. In *ICML*, pages 448–456, 2015.

- Adam Paszke, Sam Gross, Francisco Massa, Adam Lerer, James Bradbury, Gregory Chanan, Trevor Killeen, Zeming Lin, Natalia Gimelshein, Luca Antiga, Alban Desmaison, Andreas Köpf, Edward Yang, Zach DeVito, Martin Raison, Alykhan Tejani, Sasank Chilamkurthy, Benoit Steiner, Lu Fang, Junjie Bai, and Soumith Chintala. PyTorch: An Imperative Style, High-Performance Deep Learning Library. In *NeurIPS*, pages 8024–8035, 2019.
- Yang You, Igor Gitman, and Boris Ginsburg. Large Batch Training of Convolutional Networks. *arXiv:1708.03888v3 [cs.CV]*, 2017.
- Ilya Loshchilov and Frank Hutter. SGDR: Stochastic Gradient Descent with Warm Restarts. In *ICLR*,
- Ilya Sutskever, James Martens, George Dahl, and Geoffrey Hinton. On the Importance of Initialization and Momentum in Deep Learning. In *ICML*, pages 1139–1147, 2013.
- Xinlei Chen, Haoqi Fan, Ross Girshick, and Kaiming He. Improved Baselines with Momentum Contrastive Learning. *arXiv:2003.04297v1 [cs.CV]*, 2020c.
- Pascal Vincent, Hugo Larochelle, Yoshua Bengio, and Pierre-Antoine Manzagol. Extracting and Composing Robust Features with Denoising Autoencoders. In *ICML*, pages 1096–1103, 2008.
- Richard Zhang, Phillip Isola, and Alexei A. Efros. Colorful Image Colorization. In *ECCV*, pages 649–666, 2016.
- Gustav Larsson, Michael Maire, and Gregory Shakhnarovich. Learning Representations for Automatic Colorization. In *ECCV*, pages 577–593, 2016.
- Mehdi Noroozi and Paolo Favaro. Unsupervised Learning of Visual Representations by Solving Jigsaw Puzzles. In *ECCV*, pages 69–84, 2016.
- Deepak Pathak, Philipp Krähenbühl, Jeff Donahue, Trevor Darrell, and Alexei A. Efros. Context Encoders: Feature Learning by Inpainting. In *CVPR*, pages 2536–2544, 2016.
- Richard Zhang, Phillip Isola, and Alexei A. Efros. Split-Brain Autoencoders: Unsupervised Learning by Cross-Channel Prediction. In *CVPR*, pages 1058–1067, 2017.
- Spyros Gidaris, Praveer Singh, and Nikos Komodakis. Unsupervised Representation Learning by Predicting Image Rotations. In *ICLR*, 2018.
- Jeff Donahue and Karen Simonyan. Large Scale Adversarial Representation Learning. In *NeurIPS*, pages 10542–10552, 2019.
- Ryan Kiros, Yukun Zhu, Ruslan Salakhutdinov, Richard S. Zemel, Antonio Torralba, Raquel Urtasun, and Sanja Fidler. Skip-Thought Vectors. In *NeurIPS*, pages 3294–3302, 2015.
- Alexey Dosovitskiy, Philipp Fischer, Jost Tobias Springenberg, Martin Riedmiller, and Thomas Brox. Discriminative Unsupervised Feature Learning with Convolutional Neural Networks. In *NeurIPS*, pages 766–774, 2014.
- Michael U. Gutmann and Aapo Hyvärinen. Noise-Contrastive Estimation of Unnormalized Statistical Models, with Applications to Natural Image Statistics. *Journal of Machine Learning Research*, 13: 307–361, 2012.
- R Devon Hjelm, Alex Fedorov, Samuel Lavoie-Marchildon, Karan Grewal, Phil Bachman, Adam Trischler, and Yoshua Bengio. Learning Deep Representations by Mutual Information. In *ICLR*, 2019.

- Ben Poole, Sherjil Ozair, Aäron van den Oord, Alexander A. Alemi, and George Tucker. On Variational Bounds of Mutual Information. In *ICML*, pages 5171–5180, 2019.
- Ralph Linsker. Self-Organization in a Perceptual Network. Computer, 21(3):105–117, 1988.
- Geoffrey E. Hinton and Suzanna Becker. An Unsupervised Learning Procedure that Discovers Surfaces in Random-dot Stereograms. In *IJCNN*, pages 218–222, 1990.
- Michael Tschannen, Josip Djolonga, Paul K. Rubenstein, Sylvain Gelly, and Mario Lucic. On Mutual Information Maximization for Representation Learning. In *ICLR*, 2020.
- Alexander Kolesnikov, Xiaohua Zhai, and Lucas Beyer. Revisiting Self-Supervised Visual Representation Learning. In *CVPR*, pages 1920–1929, 2019.
- David McAllester and Karl Stratos. Formal Limitations on the Measurement of Mutual Information. In *AISTATS*, pages 875–884, 2020.
- Yamini Bansal, Gal Kaplun, and Boaz Barak. For Self-Supervised Learning, Rationality Implies Generalization, Provably. In *ICLR*, 2021.
- Tongzhou Wang and Phillip Isola. Understanding Contrastive Representation Learning through Alignment and Uniformity on the Hypersphere. In *ICML*, pages 9929–9939, 2020.
- Christopher Tosh, Akshay Krishnamurthy, and Daniel Hsu. Contrastive Learning, Multi-view Redundancy, and Linear Models. *arXiv:2008.10150v1 [cs.LG]*, 2020.
- Colin Wei, Kendrick Shen, Yining Chen, and Tengyu Ma. Theoretical Analysis of Self-Training with Deep Networks on Unlabeled Data. In *ICLR*, 2021.
- Jason D. Lee, Qi Lei, Nikunj Saunshi, and Jiacheng Zhuo. Predicting What You Already Know Helps: Provable Self-Supervised Learning. *arXiv*:2008.01064v1 [cs.LG], 2020.
- Nikunj Saunshi, Sadhika Malladi, and Sanjeev Arora. A Mathematical Exploration of Why Language Models Help Solve Downstream Tasks. In *ICLR*, 2021.
- Shuxiao Chen, Edgar Dobriban, and Jane H. Lee. A Group-Theoretic Framework for Data Augmentation. *Journal of Machine Learning Research*, 21:1–71, 2020d.
- Philippe Flajolet, Danièle Gardy, and Loÿs Thimonier. Birthday Paradox, Coupon Collectors, Caching Algorithms and Self-organizing Search. *Discrete Applied Mathematics*, 39(3):207–229, 1992.

# **A** The Proofs

# A.1 The Inequality in Eq. (7)

We show the following inequality:

$$\mathbb{E}_{\substack{c, \{c_{k}^{-}\}_{k=1}^{K} \sim \rho^{K+1} \\ \mathbf{x} \sim \mathcal{D}_{c} \\ \mathbf{a} \sim \mathcal{A}}} \ell_{\text{Info}}\left(\mathbf{z}, \left\{\boldsymbol{\mu}(\mathbf{x}), \boldsymbol{\mu}_{c_{1}^{-}}, \dots, \boldsymbol{\mu}_{c_{K}^{-}}\right\}\right) \geq \mathbb{E}_{\substack{c, \{c_{k}^{-}\}_{k=1}^{K} \sim \rho^{K+1} \\ \mathbf{x} \sim \mathcal{D}_{c} \\ \mathbf{a} \sim \mathcal{A}}} \ell_{\text{Info}}\left(\mathbf{z}, \left\{\boldsymbol{\mu}_{c}, \boldsymbol{\mu}_{c_{1}^{-}}, \dots, \boldsymbol{\mu}_{c_{K}^{-}}\right\}\right) + d(\mathbf{f}).$$
(14)

*Proof.* We replace  $\mu(\mathbf{x})$  with  $\mu_c$  in the left hand side:

$$\mathbb{E}_{c,\{c_{k}^{-}\}_{k=1}^{K} \sim \rho^{K+1}} \ell_{Info} \left( \mathbf{z}, \left\{ \boldsymbol{\mu}(\mathbf{x}), \boldsymbol{\mu}_{c_{1}^{-}}, \dots, \boldsymbol{\mu}_{c_{K}^{-}} \right\} \right) \\
\times \sim \mathcal{D}_{c} \\
\mathbf{a} \sim \mathcal{A}$$

$$= \mathbb{E}_{c,\{c_{k}^{-}\}_{k=1}^{K} \sim \rho^{K+1}} \ell_{Info} \left( \mathbf{z}, \left\{ \boldsymbol{\mu}(\mathbf{x}), \boldsymbol{\mu}_{c_{1}^{-}}, \dots, \boldsymbol{\mu}_{c_{K}^{-}} \right\} \right) \\
+ \mathbb{E}_{c,\{c_{k}^{-}\}_{k=1}^{K} \sim \rho^{K+1}} \ell_{Info} \left( \mathbf{z}, \left\{ \boldsymbol{\mu}_{c}, \boldsymbol{\mu}_{c_{1}^{-}}, \dots, \boldsymbol{\mu}_{c_{K}^{-}} \right\} \right) - \mathbb{E}_{c,\{c_{k}^{-}\}_{k=1}^{K} \sim \rho^{K+1}} \ell_{Info} \left( \mathbf{z}, \left\{ \boldsymbol{\mu}_{c}, \boldsymbol{\mu}_{c_{1}^{-}}, \dots, \boldsymbol{\mu}_{c_{K}^{-}} \right\} \right) \\
= \mathbb{E}_{c,\{c_{k}^{-}\}_{k=1}^{K} \sim \rho^{K+1}} \ell_{Info} \left( \mathbf{z}, \left\{ \boldsymbol{\mu}_{c}, \boldsymbol{\mu}_{c_{1}^{-}}, \dots, \boldsymbol{\mu}_{c_{K}^{-}} \right\} \right) \\
\times \sim \mathcal{D}_{c} \\
\mathbf{a} \sim \mathcal{A}$$

$$+ \mathbb{E}_{c,\{c_{k}^{-}\}_{k=1}^{K} \sim \rho^{K+1}} \left[ \ell_{Info} \left( \mathbf{z}, \left\{ \boldsymbol{\mu}(\mathbf{x}), \boldsymbol{\mu}_{c_{1}^{-}}, \dots, \boldsymbol{\mu}_{c_{K}^{-}} \right\} \right) - \ell_{Info} \left( \mathbf{z}, \left\{ \boldsymbol{\mu}_{c}, \boldsymbol{\mu}_{c_{1}^{-}}, \dots, \boldsymbol{\mu}_{c_{K}^{-}} \right\} \right) \right] . \tag{15}$$

$$+ \mathbb{E}_{c,\{c_{k}^{-}\}_{k=1}^{K} \sim \rho^{K+1}} \left[ \ell_{Info} \left( \mathbf{z}, \left\{ \boldsymbol{\mu}(\mathbf{x}), \boldsymbol{\mu}_{c_{1}^{-}}, \dots, \boldsymbol{\mu}_{c_{K}^{-}} \right\} \right) - \ell_{Info} \left( \mathbf{z}, \left\{ \boldsymbol{\mu}_{c}, \boldsymbol{\mu}_{c_{1}^{-}}, \dots, \boldsymbol{\mu}_{c_{K}^{-}} \right\} \right) \right] . \tag{15}$$

When the gap term is non-negative:  $\mathbf{z} \cdot \boldsymbol{\mu}(\mathbf{x}) \leq \mathbf{z} \cdot \boldsymbol{\mu}_c$ , we simply drop it in Eq. (15) to obtain the bound. Thus we consider a lower bound of the gap term when the gap term is negative,  $\mathbf{z} \cdot \boldsymbol{\mu}(\mathbf{x}) > \mathbf{z} \cdot \boldsymbol{\mu}_c$ , to guarantee Eq. (15). As a general case, we show the bound with temperature parameter t.

The gap term in Eq. (15) = 
$$\underset{\mathbf{z} \sim \mathcal{D}_{c}}{\mathbb{E}} \underbrace{\sum_{\substack{k=1 \ \mathbf{x} \sim \mathcal{D}_{c} \\ \mathbf{x} \sim \mathcal{D}_{c} \\ \mathbf{x} \sim \mathcal{D}_{c}}} \left[ \mathbf{z} \cdot (\boldsymbol{\mu}_{c} - \boldsymbol{\mu}(\mathbf{x}))/t \right] + \underbrace{\ln \frac{\exp \left( \mathbf{z} \cdot \boldsymbol{\mu}(\mathbf{x})/t \right) + \sum_{k=1}^{K} \exp \left( \mathbf{z} \cdot \boldsymbol{\mu}_{c_{k}}/t \right)}{\exp \left( \mathbf{z} \cdot \boldsymbol{\mu}_{c}/t \right) + \sum_{k=1}^{K} \exp \left( \mathbf{z} \cdot \boldsymbol{\mu}_{c_{k}}/t \right)}$$

$$> \underbrace{\mathbb{E}}_{\mathbf{x} \sim \mathcal{D}_{c}} \left[ \mathbb{E}_{\mathbf{x} \sim \mathcal{A}} \left[ \mathbf{f}(\mathbf{a}(\mathbf{x})) \right] \cdot \left( \mathbb{E}_{\mathbf{x}' \sim \mathcal{D}_{c}} \left[ \mathbf{f}(\mathbf{a}'(\mathbf{x}')) \right] - \mathbb{E}_{\mathbf{a}'' \sim \mathcal{A}} \left[ \mathbf{f}(\mathbf{a}''(\mathbf{x})) \right] \right) / t \right]$$

$$= \frac{1}{t} \underbrace{\mathbb{E}}_{c \sim \rho} \left[ \|\boldsymbol{\mu}_{c}\|_{2}^{2} - \mathbb{E}_{\mathbf{x} \sim \mathcal{D}_{c}} \|\boldsymbol{\mu}(\mathbf{x})\|_{2}^{2} \right]$$

$$:= d(\mathbf{f}).$$

$$(16)$$

# A.2 The Proof of Proposition 6

We apply the proof of Theorem B.1 in Arora et al. [2019] to our setting.

*Proof.* We start from Eq. (7).

$$(7) = (1 - \tau_{K}) \underset{\substack{c, \{c_{k}^{-}\}_{k=1}^{K} \sim \rho^{K+1} \\ \mathbf{x} \sim \mathcal{D}_{c} \\ \mathbf{a} \sim \mathcal{A}}}{\mathbb{E}} \left[ \left[ \ell_{\text{Info}} \left( \mathbf{z}, \left\{ \boldsymbol{\mu}_{c}, \boldsymbol{\mu}_{c_{1}^{-}}, \dots, \boldsymbol{\mu}_{c_{K}^{-}} \right\} \right) \mid \text{Col} = 0 \right] \right]$$

$$+ \tau_{K} \underset{\substack{x \sim \mathcal{D}_{c} \\ \mathbf{x} \sim \mathcal{D}_{c} \\ \mathbf{a} \sim \mathcal{A}}}{\mathbb{E}} \left[ \ell_{\text{Info}} \left( \mathbf{z}, \left\{ \boldsymbol{\mu}_{c}, \boldsymbol{\mu}_{c_{1}^{-}}, \dots, \boldsymbol{\mu}_{c_{K}^{-}} \right\} \right) \mid \text{Col} \neq 0 \right] + d(\mathbf{f})$$

$$\geq (1 - \tau_{K}) \underset{\substack{x \sim \mathcal{D}_{c} \\ \mathbf{a} \sim \mathcal{A}}}{\mathbb{E}} \left[ \ell_{\text{sub}}^{\mu} (\mathbf{z}, c, \mathcal{C}_{\text{sub}}) \mid \text{Col} = 0 \right]$$

$$\xrightarrow{x \sim \mathcal{D}_{c}} \underset{\mathbf{a} \sim \mathcal{A}}{\mathbb{E}} \left[ \ell_{\text{sub}}^{\mu} (\mathbf{z}, c, \{c_{s}^{\text{Col}+1}) \mid \text{Col} \neq 0 \right] + d(\mathbf{f})$$

$$= (1 - \tau_{K}) \underset{\substack{x \sim \mathcal{D}_{c} \\ \mathbf{a} \sim \mathcal{A}}}{\mathbb{E}} \left[ L_{\text{sub}}^{\mu} (\mathbf{z}, \mathcal{C}_{\text{sub}}) \mid \text{Col} = 0 \right] + \tau_{K} \underset{\substack{c, \{c_{k}^{-}\}_{k=1}^{K} \sim \rho^{K+1}}}{\mathbb{E}} \left[ \ln(\text{Col} + 1) \mid \text{Col} \neq 0 \right] + d(\mathbf{f}),$$

$$= (1 - \tau_{K}) \underset{\substack{c, \{c_{k}^{-}\}_{k=1}^{K} \sim \rho^{K+1}}}{\mathbb{E}} \left[ L_{\text{sub}}^{\mu} (\mathbf{z}, \mathcal{C}_{\text{sub}}) \mid \text{Col} = 0 \right] + \tau_{K} \underset{\substack{c, \{c_{k}^{-}\}_{k=1}^{K} \sim \rho^{K+1}}}{\mathbb{E}} \left[ \ln(\text{Col} + 1) \mid \text{Col} \neq 0 \right] + d(\mathbf{f}),$$

$$= (17)$$

where  $\{c\}^{\mathrm{Col}+1}$  is a bag of latent classes such that only c appears  $\mathrm{Col}+1$  times. The first decomposition is done by using collision probability  $\tau_K$  conditioned on  $\mathrm{Col}$ . The inequality is obtained by removing duplicated latent classes from the first term and removing the other latent classes from the second term. Note that InfoNCE is a monotonically increasing function; its value decreases by removing any elements in the negative samples of the loss.

### A.3 The Proof of Theorem 8

*Proof.* We start from Eq. (7).

$$(7) = v_{K+1} \underset{\mathbf{z}, \{c_{k}^{-}\}_{k=1}^{K} \sim \rho^{K+1}}{\mathbb{E}} \left[ \ell_{\text{Info}} \left( \mathbf{z}, \left\{ \boldsymbol{\mu}_{c}, \boldsymbol{\mu}_{c_{1}^{-}}, \dots, \boldsymbol{\mu}_{c_{K}^{-}} \right\} \right) \mid \mathcal{C}_{\text{sub}} = \mathcal{C} \right]$$

$$+ (1 - v_{K+1}) \underset{\mathbf{z}, \mathcal{D}_{c}}{\mathbb{E}} \underset{\mathbf{z} \sim \mathcal{D}_{c}}{\mathbb{E}} \left[ \ell_{\text{Info}} \left( \mathbf{z}, \left\{ \boldsymbol{\mu}_{c}, \boldsymbol{\mu}_{c_{1}^{-}}, \dots, \boldsymbol{\mu}_{c_{K}^{-}} \right\} \right) \mid \mathcal{C}_{\text{sub}} \neq \mathcal{C} \right] + d(\mathbf{f})$$

$$\geq \frac{1}{2} \left\{ v_{K+1} \underset{\mathbf{z} \sim \mathcal{D}_{c}}{\mathbb{E}} \underset{\mathbf{z} \sim \mathcal{D}_{c}}{\mathbb{E}} \left[ \ell_{\text{sub}}^{\mu} (\mathbf{z}, c, \mathcal{C}_{\text{sub}}) \mid \mathcal{C}_{\text{sub}} = \mathcal{C} \right] \right.$$

$$+ (1 - v_{K+1}) \underset{\mathbf{z} \sim \mathcal{D}_{c}}{\mathbb{E}} \underset{\mathbf{z} \sim \mathcal{D}_{c}}{\mathbb{E}} \left[ \ell_{\text{sub}}^{\mu} (\mathbf{z}, c, \mathcal{C}_{\text{sub}}) \mid \mathcal{C}_{\text{sub}} \neq \mathcal{C} \right]$$

$$+ \left. \mathbb{E} \underset{c, \{c_{k}^{-}\}_{k=1}^{K} \sim \rho^{K+1}}{\mathbb{E}} \ln(\text{Col} + 1) \right\} + d(\mathbf{f}).$$

$$(19)$$

The first decomposition is obtained by using the definition of v to distinguish whether or not the sampled latent classes contain all latent classes C. To derive the inequality, we use the following properties

of the cross-entropy loss. Fixed f and c, for all  $K \subseteq \{1, ..., K\}$ , the value of  $\ell_{\text{Info}}$  holds the following inequality:

$$\ell_{\text{Info}}\left(\mathbf{z}, \left\{\boldsymbol{\mu}_{c}, \boldsymbol{\mu}_{c_{1}^{-}}, \dots, \boldsymbol{\mu}_{c_{K}^{-}}\right\}\right) \geq \ell_{\text{Info}}\left(\mathbf{z}, \left\{\boldsymbol{\mu}_{c}, \boldsymbol{\mu}_{c_{k}^{-}}\right\}_{k \in \mathcal{K}}\right). \tag{20}$$

Thus we apply the following inequalities to the first and second terms in Eq. (18).

$$\ell_{\text{Info}}\left(\mathbf{z}, \left\{\boldsymbol{\mu}_{c}, \boldsymbol{\mu}_{c_{1}^{-}}, \dots, \boldsymbol{\mu}_{c_{K}^{-}}\right\}\right) \geq \frac{1}{2} \left[\ell_{\text{sub}}^{\mu}\left(\mathbf{z}, c, \mathcal{C}_{\text{sub}}\right) + \ell_{\text{sub}}^{\mu}\left(\mathbf{z}, c, \left\{c\right\}^{\text{Col}+1}\right)\right]$$

$$= \frac{1}{2} \left[\ell_{\text{sub}}^{\mu}\left(\mathbf{z}, c, \mathcal{C}_{\text{sub}}\right) + \ln(\text{Col}+1)\right]$$
(21)

By rearranging Eq. (19), we obtain the lower bound in Theorem 8.

# A.4 The Proof of Corollary 10

We prove Corollary 10 that shows the upper bound of the collision term to understand the effect of the number of negative samples. Our proof is inspired by Arora et al. [2019, Lemma A.1.]. As a general case, we consider the loss function with temperature parameter t.

*Proof.* We decompose the self-supervised loss  $L_{\rm Info}$  by using v to extract the collision term.

$$L_{Info}(\mathbf{f})$$

$$=v_{K+1}\begin{bmatrix} \mathbb{E} & \mathbb{E} & \mathbb{E} & \mathbb{E} \\ c_{:}\{c_{k}^{\top}\}_{k=1}^{K} \sim \rho^{K+1} & \mathbb{E}^{\times \mathcal{D}_{c}} \{\mathbf{x}_{k}^{\top} \sim \mathcal{D}_{c-k}^{\top}\}_{k=1}^{K} \\ \{\mathbf{a}_{k}^{\top}\}_{k=1}^{K} \sim A^{K}} \end{bmatrix} \left[ \ell_{Info}(\mathbf{z}, \mathbf{Z}) \mid \mathcal{C}_{sub} = \mathcal{C} \right]$$

$$+ (1 - v_{K+1}) \begin{bmatrix} \mathbb{E} & \mathbb{E} & \mathbb{E} \\ c_{:}\{c_{k}^{\top}\}_{k=1}^{K} \sim \rho^{K+1} & \mathbb{E}^{\times \mathcal{D}_{c}} \{\mathbf{x}_{k}^{\top} \sim \mathcal{D}_{c-k}^{\top}\}_{k=1}^{K} \\ \mathbf{a}_{k}^{\top} \sim A^{K}} \end{bmatrix} \left[ \ell_{Info}(\mathbf{z}, \mathbf{Z}) \mid \mathcal{C}_{sub} \neq \mathcal{C} \right]$$

$$\leq v_{K+1} \begin{bmatrix} \mathbb{E} & \mathbb{E} & \mathbb{E} \\ c_{:}\{c_{k}^{\top}\}_{k=1}^{K} \sim \rho^{K+1} & \mathbb{E}^{\times \mathcal{D}_{c}} \{\mathbf{a}_{k}^{\top}\}_{k=1}^{K} \sim A^{K}} \end{bmatrix} \left[ \ell_{Info}(\mathbf{z}, \{\mathbf{z}_{k}\}_{c \neq c_{k}^{\top}}) + \ell_{Info}(\mathbf{z}, \{\mathbf{z}_{k}\}_{c = c_{k}^{\top}}) \mid \mathcal{C}_{sub} = \mathcal{C} \right]$$

$$+ (1 - v_{K+1}) \begin{bmatrix} \mathbb{E} & \mathbb{E} & \mathbb{E} \\ c_{:}\{c_{k}^{\top}\}_{k=1}^{K} \sim \rho^{K+1} & \mathbb{E}^{\times \mathcal{D}_{c}} \{\mathbf{a}_{k}^{\top}\}_{k=1}^{K} \sim \mathcal{D}_{c_{k}^{\top}}\}_{k=1}^{K} \end{bmatrix} \left[ \ell_{Info}(\mathbf{z}, \{\mathbf{z}_{k}\}_{c \neq c_{k}^{\top}}) + \ell_{Info}(\mathbf{z}, \{\mathbf{z}_{k}\}_{c = c_{k}^{\top}}) \mid \mathcal{C}_{sub} \neq \mathcal{C} \right]$$

$$= \mathbb{E} & \mathbb{E} & \mathbb{E} & \ell_{Info}(\mathbf{z}, \{\mathbf{z}_{k}\}_{c = c_{k}^{\top}}) + \mathrm{Reminder}$$

$$= \mathbb{E} \mathcal{E} \mathcal{E} \times \mathcal{E}_{c_{k}^{\top}} \mathcal{E}_{k=1}^{C_{ol+1}} \mathcal{D}_{c_{k}^{\top}}^{C_{ol+1}} \mathcal{E}_{k=1}^{C_{ol+2}} \mathcal{E}_{k=1$$

Table 4: The expected number of samples to draw all supervised classes.

Dataset	# classes	$\mathbb{E}[K+1]$
CIFAR-10	10	30
CIFAR-100	100	519
ImageNet	1000	7709

where  $\mathcal{B}_c$  is the probability distribution over Col conditioned on c. The first equality is done by decomposition with v. The inequality is obtained by using the following property of the cross-entropy loss. Given  $\mathcal{K} \subseteq \{1, \ldots, K\}$ ,

$$\ell_{\text{Info}}(\mathbf{z}, \mathbf{Z}) \le \ell_{\text{Info}}(\mathbf{z}, \{\mathbf{z}_k\}_{k \in \mathcal{K}}) + \ell_{\text{Info}}(\mathbf{z}, \{\mathbf{z}_k\}_{k \in \{1, \dots, K\} \setminus \mathcal{K}}). \tag{23}$$

We focus on the first term in Eq. (22), where the loss takes samples such that they have the same latent class c. Fixed  $\mathbf{f}$  and c, let  $M = \max_{\mathbf{z}_k \in \mathbf{Z}} \mathbf{z} \cdot \mathbf{z}_k / t$ , and  $\mathbf{z}^* = \operatorname{argmax}_{\mathbf{z}_k \in \mathbf{Z}} \mathbf{z} \cdot \mathbf{z}_k$ .

$$\mathbb{E}_{\substack{c \sim \rho \\ \text{Col} \sim \mathcal{B}_{c}}} \mathbb{E}_{\mathbf{x}, \{\mathbf{x}_{k}^{-}\}_{k=1}^{\text{Col}} \sim \mathcal{D}_{c}^{\text{Col}+1}}} \ell_{\text{Info}}(\mathbf{z}, \mathbf{Z}) \leq \mathbb{E}_{\substack{c \sim \rho \\ \text{Col} \sim \mathcal{B}_{c}}} \mathbb{E}_{\mathbf{x}, \{\mathbf{x}_{k}^{-}\}_{k=1}^{\text{Col}} \sim \mathcal{D}_{c}^{\text{Col}+1}}} -\mathbf{z} \cdot \mathbf{z}'/t + \ln\left[\exp(\mathbf{z} \cdot \mathbf{z}'/t) + \text{Col}\exp(M)\right]$$

$$\leq \mathbb{E}_{\substack{c \sim \rho \\ \text{Col} \sim \mathcal{B}_{c}}} \mathbb{E}_{\mathbf{x}, \{\mathbf{x}_{k}^{-}\}_{k=1}^{\text{Col}} \sim \mathcal{D}_{c}^{\text{Col}+1}}} \max\left[\ln(\text{Col} + 1), \ln(\text{Col} + 1) - \mathbf{z} \cdot \mathbf{z}'/t + M\right]$$

$$\leq \mathbb{E}_{\substack{c \sim \rho \\ \text{Col} \sim \mathcal{B}_{c}}} \mathbb{E}_{\mathbf{x}, \{\mathbf{x}_{k}^{-}\}_{k=1}^{\text{Col}} \sim \mathcal{D}_{c}^{\text{Col}+1}}$$

$$\leq \mathbb{E}_{\substack{c \sim \rho \\ \text{Col} \sim \mathcal{B}_{c}}} \mathbb{E}_{\mathbf{x}, \{\mathbf{x}_{k}^{-}\}_{k=1}^{\text{Col}} \sim \mathcal{D}_{c}^{\text{Col}+1}}$$

$$\leq \mathbb{E}_{\substack{c \sim \rho \\ \text{Col} \sim \mathcal{B}_{c}}} \mathbb{E}_{\mathbf{x}, \{\mathbf{x}_{k}^{-}\}_{k=1}^{\text{Col}} \sim \mathcal{D}_{c}^{\text{Col}+1}}$$

$$\leq \mathbb{E}_{\substack{c \sim \rho \\ \text{Col} \sim \mathcal{B}_{c}}} \mathbb{E}_{\mathbf{x}, \{\mathbf{x}_{k}^{-}\}_{k=1}^{\text{Col}} \sim \mathcal{D}_{c}^{\text{Col}+1}}$$

$$\leq \mathbb{E}_{\substack{c \sim \rho \\ \text{Col} \sim \mathcal{B}_{c}}} \mathbb{E}_{\mathbf{x}, \{\mathbf{x}_{k}^{-}\}_{k=1}^{\text{Col}} \sim \mathcal{D}_{c}^{\text{Col}+1}}$$

$$\leq \mathbb{E}_{\substack{c \sim \rho \\ \text{Col} \sim \mathcal{B}_{c}}} \mathbb{E}_{\mathbf{x}, \{\mathbf{x}_{k}^{-}\}_{k=1}^{\text{Col}} \sim \mathcal{D}_{c}^{\text{Col}+1}}$$

$$\leq \mathbb{E}_{\substack{c \sim \rho \\ \text{Col} \sim \mathcal{B}_{c}}} \mathbb{E}_{\mathbf{x}, \{\mathbf{x}_{k}^{-}\}_{k=1}^{\text{Col}} \sim \mathcal{D}_{c}^{\text{Col}+1}}$$

$$\leq \mathbb{E}_{\mathbf{x}, \{\mathbf{x}_{k}^{-}\}_{k=1}^{\text{Col}} \sim \mathcal{D}_{c}^{\text{Col}$$

Note that  $\ln(\operatorname{Col} + 1)$  is the constant depending on the number of duplicated latent class, then we focus on  $\|\mathbf{z} \cdot \mathbf{z}^* - \mathbf{z} \cdot \mathbf{z}'\|_1$ .

$$\underset{\substack{\mathbf{x}, \{\mathbf{x}_k^-\}_{k=1}^{\mathrm{Col}} \sim \mathcal{D}_c^{\mathrm{Col}+1} \\ \mathbf{a}, \mathbf{a}', \{\mathbf{a}_k^-\}_{k=1}^{\mathrm{Col}} \sim \mathcal{A}^{\mathrm{Col}+2} }}{\mathbb{E}} |\mathbf{z} \cdot \mathbf{z}^* - \mathbf{z} \cdot \mathbf{z}'| \leq \left(\mathrm{Col} + 1\right) \underbrace{\underset{\substack{\mathbf{x} \sim \mathcal{D}_c \\ \mathbf{a}, \mathbf{a}' \sim \mathcal{A}^2}}{\mathbb{E}}}_{\substack{\mathbf{x}^- \sim \mathcal{D}_c \\ \mathbf{a}^- \sim \mathcal{A}}} |\mathbf{z} \cdot \mathbf{z}^- - \mathbf{z} \cdot \mathbf{z}'|.$$

Therefore,  $\alpha = \ln(\text{Col} + 1)$ , and  $\beta = \frac{\text{Col} + 1}{t}$ .

# B Expected Number of Negative Samples to Draw all Supervised Labels

We assume that we can sample a latent class from  $\rho$  independently, and let  $\rho(c) \in [0,1]$  be a probability that c is sampled. Flajolet et al. [1992, Theorem 4.1] show the expected number K+1 to sample all latent class in  $\mathcal C$  is defined by

$$\mathbb{E}[K+1] = \int_0^\infty \left(1 - \prod_{c \in \mathcal{C}} [1 - \exp(-\rho(c)x)]\right) \mathrm{d}x. \tag{25}$$

Table 4 shows the expected number of sampled latent classes on a popular classification dataset when the latent class is the same as the supervised class. Recent instance discriminative self-supervised learning on the ImageNet-1K dataset [Deng et al., 2009], where  $Y=1\,000$ . Thus, the empirical number of negative samples is supposed to be natural, for example,  $K\geq 8\,096$  in experiments by Chen et al. [2020a], He et al. [2020] because the expected number of latent classes to draw all supervised classes is about  $7\,709$ .